Catena 141 (2016) 66–72

Contents lists available at ScienceDirect

Catena

journal homepage: www.elsevier.com/locate/catena

Dynamics of soil aggregate size in turbulent flow: Respective effect of soil type and suspended concentration

Valentin Wendling [a,*], Cédric Legout [a], Nicolas Gratiot [b], Hervé Michallet [c], Thomas Grangeon [d,e]

[a] Université Grenoble Alpes, LTHE, BP 53, 38041 Grenoble Cedex 09, France
[b] IRD, LTHE, BP 53, 38041 Grenoble Cedex 09, France
[c] CNRS, LEGI UMR 5519, Grenoble, France
[d] EA 6293 GéoHydrosystèmes Continentaux, Université François Rabelais, Faculté des Sciences et Techniques, Parc de Grandmont, 37200 Tours, France
[e] Bureau de Recherche Géologiques et Minières, Département Risques et Préventions, 3 avenue Claude Guillemin, 45060 Orléans, France

A R T I C L E   I N F O

Article history:
Received 27 July 2015
Received in revised form 11 February 2016
Accepted 17 February 2016
Available online 3 March 2016

Keywords:
Soil erosion
Aggregates
Suspended sediment dynamics
Disaggregation
Sediment transport
Particle size distribution

A B S T R A C T

The fate of eroded soil particles impacts soil loss, river engineering and aquatic ecosystems. However, little is known about soil aggregate dynamics within the flow just after their detachment from the soil matrix. The relationship between particle size and turbulence has already been studied but few studies analysed the associated effect of particle concentration. The disaggregation/flocculation of three soils, two badland materials and a well developed calcareous brown soil, was studied by using a grid-stirred tank. An isotropic and homogeneous turbulence was generated to focus on the effects of suspended concentration on particle sizes. Increasing the suspended concentration in the range $1-10$ g L^{-1} leads to a decrease of the proportion of the medium size particles and of an increase of the proportion of the smallest particles, as a consequence to enhanced abrasion. The soil aggregates with the largest organic content had the highest strength but were still subject to disaggregation within the turbulent flow, the resulting particle size depending on the suspended concentration. This study demonstrates that soil aggregate characteristics are influenced by concentration, this behaviour being dependent upon the soil type.

1. Introduction

Soil erosion by water is considered to be the main threat to soils in Europe. The concerning extent of 10^6 km^2 of eroded soils (Jones et al., 2012), 16% of Europe's total land area, is expected to increase in the context of global change. In addition to local land degradation resulting in net loss in crop productivity (Collins et al., 2005), the transfer of sediments to rivers is also of great concern for aquatic life and water resources (Owens et al., 2005). It contributes to reservoir siltation and to the export of pollutants such as heavy metals and nutrients to downstream water bodies. Despite modelling efforts undertaken in the last decades, the performance of erosion models remain moderate to low (Jetten et al., 1999, 2003; Boardman, 2006; De Vente et al., 2013). These models therefore cannot be used as tools to evaluate erosion mitigation strategies or the evolution of sediment yield in a context of climatic change.

Wainwright et al. (2008) pointed out that the inability of catchment scale models to correctly reproduce soil erosion could be related to their inability to consider particle travel distances. The maintenance of solid particles in suspension results from the balance between turbulence and particle settling velocity (Winterwerp, 2001). As the settling velocity is mainly dependent on particle sizes, one of the possible misconceptions of mechanistic erosion models may be due to the fact that particle sizes are considered to be stable over time after their detachment from the soil matrix. Conversely, in the conceptual models developed for lowland rivers and estuarine environments, such as the ones proposed by Dyer (1989) or Droppo (2004), it is considered that the particle sizes are mostly controlled by in-channel processes acting upon the suspended particles, i.e. flocculation and disaggregation, each being dependent upon particle concentration and flow turbulence. Headwater hydrosystems are characterized by a high temporal variability of discharges, suspended concentrations (Navratil et al., 2012) and suspended particle sizes (Grangeon et al., 2012). This emphasizes the need to study the effects of turbulence and suspended concentration on soil particles. While particles eroded from the soil matrix are mainly aggregated particles, almost no studies have addressed the dynamic behaviour of soil aggregates within headwater hydrosystems. It was however demonstrated that soil aggregates seem to coexist with newly formed flocs during runoff events (Droppo et al., 2005; Williams et al., 2008). Grangeon et al. (2014) explored this issue through laboratory experiments for three soils within an annular flume. Over an increasing and decreasing sequence of bed shear stress, their observations suggest that soil aggregates were not stable once introduced in the flow, but rather undergo disaggregation and flocculation. Large

* Corresponding author.
E-mail addresses: valentin.wendling@gmail.com (V. Wendling), Cedric.legout@ujf-grenoble.fr (C. Legout), nicolas.gratiot@ird.fr (N. Gratiot), herve.michallet@legi.cnrs.fr (H. Michallet), t.grangeon@brgm.fr (T. Grangeon).

http://dx.doi.org/10.1016/j.catena.2016.02.015
0341-8162/

differences in particle size were found between soils during the early stage of the rising limb of the bed shear stress sequence. The differences were smaller in the falling limb suggesting that soil aggregates underwent structural change. However, the intrinsic design of the flume experiments did not allow for dissociating the respective effects of flow turbulence and suspended concentration on particle characteristics, as both varied during experiments due to bed erosion and deposition. The objectives of the present study were therefore to assess i) how the suspended concentration impacts soil aggregate sizes and ii) whether concentration plays a lesser or greater role than the eroded soil type.

2. Materials and methods

2.1. Soil characteristics

The dynamics of soil particles within the flow was explored through the introduction of various amounts of three soils in a turbulent water tank. The three soil types were similar to those studied by Grangeon et al. (2014). They were sampled in the first top 10 cm of bare soil areas. Two of them were collected within the Galabre catchment, located in a sedimentary area of the southern French Alps (Navratil et al., 2012). The Galabre catchment, typical of highly energetic headwater catchment, exhibited high variations of suspended sediment concentrations during runoff events (i.e. from a few g L^{-1} to more than 100 g L^{-1}) (Navratil et al., 2011; Grangeon et al., 2012; Legout et al., 2013). These two materials could not be considered as evolved soils, since they were sampled in badland areas. Therefore they were labelled with the names of the lithological layers they were originated from: black marls and molasses. The third material was collected in a sedimentary area located in southern France within the Cevennes-Vivarais Mediterranean Hydrometeorological Observatory (Boudevillain et al., 2011). It was a cultivated well-developed calcareous brown soil (Le Bissonnais et al., 2007), hereafter referred as clay soil. As shown in Table 1, the clay soil had the highest organic content. All these materials were air dried and sieved using a 1 mm mesh before the experiments.

2.2. The grid stirred tank

The experiments were conducted in a grid stirred tank. The tank is a square plexiglass box 53 cm wide and 90 cm high. The grid is made of seven square 1.5 cm bars, with a mesh size of 7.5 cm. It is fixed horizontally on a vertical bar that serves as a guide for stirring. The grid oscillates with a stroke (twice the amplitude) $S = 4.3$ cm and at a controlled frequency $f = 4$ Hz. The mean grid position is located at $h_g = 5$ cm above the bottom of the tank, and the z axis is defined upward with the origin O at the mean grid position (Fig. 1). Additional description of the experimental set-up can be found in Gratiot and Manning (2004) and Gratiot et al. (2005).

The grid stirred tank device generates a homogeneous and isotropic turbulence with an intensity depending only on the distance to the oscillating grid (Hopfinger and Toly, 1976). Matsunaga et al. (1999) proposed universal laws of turbulence decay with the distance to the grid for clear water (without sediment). Michallet and Mory (2004) later used a k–ε model (including equations for the turbulent kinetic energy k and the dissipation rate of turbulent kinetic energy ε) to study steady states of fine sediment suspensions in oscillating grid turbulence. They showed that the turbulence abruptly vanishes at some distance above the grid, leading to the formation of a sharp concentration interface called lutocline. Gratiot et al. (2005) experimentally confirmed that there is very little stratification below the lutocline. The dissipation gradient of turbulence $G = \sqrt{\varepsilon/\nu}$, where ν is the fluid kinematic viscosity, has been evaluated by Gratiot and Manning (2004) for similar experimental conditions, reaching an order of magnitude of 100 s^{-1} close to the grid and decreasing to 19, 7 and 3 s^{-1} for distances of 15, 20 and 25 cm respectively. Those values are typical of many natural flows and laboratory devices (Jarvis et al., 2005).

2.3. Experimental protocol

A set of 12 experiments were performed (Table 2). For each soil, three different amounts of material were introduced in the tank in order to maintain different levels of concentration ranging from 1.6 to 10.9 g L^{-1}. The tank was first filled ($H = 40$ cm) with tap water and the grid stirring was started. Dry material was then introduced at the top of the tank at time $t = 0$ min and the experiment lasted 40 min. Two 1 m long vinyl flexible hoses were installed at $z = 15$ cm allowing to collect simultaneously by gravity two suspended sediment samples. This sampling position has been chosen to be far enough from the grid to minimize local convection effects and to remain under the lutocline for all the experiments. Samplings were done at $t = 1$, 5, 10, 20 and 40 min. Each sampling lasted 20 s. At the end of each experiment (after 40 min) the vinyl hoses were lifted at $z = 20$ cm and $z = 25$ cm and additional samples were collected in order to evaluate potential stratification effects. For each time and position, one sample was used to measure the suspended concentration and the other one was used to measure particle size distributions (PSDs) by laser diffraction.

2.4. Measurements

Samples were weighed after collection, oven dried at 105 °C for 24 h and then reweighed in order to measure the suspended sediment concentration (SSC). The position of the lutocline z_l above the central position of the grid was visually tracked during each experiment, as done by Gratiot et al. (2005). Particle size distributions (PSDs) were measured with a laser diffraction sizer (Malvern, Mastersizer 2000) operating in the range 0.01 − 2000 μm. An equivalent spherical volume hypothesis is considered to calculate PSD from the diffraction data (Andrews et al., 2010). In case of elongated or complex particle shapes, the laser sizer device measures both the small and large axes of the particles and an equivalent volume is attribute to both sizes (Graham et al., 2012). For each sample, a first PSD measurement, referred as to the aggregated PSD, was performed during the first thirty seconds without sonication and with stirring and pumping at half of their maximum levels (i.e. 500 and 1250 rpm respectively). This procedure was developed and validated by Grangeon et al. (2012, 2014) to minimize sample disturbance. Then sonication was activated, stirring and pumping were increased at their maximum levels. PSD was then measured each minute to record the disaggregation dynamics. The measurement performed after 10 min was assumed to be the dispersed PSD corresponding to physical dispersion. This duration corresponds to the time to which maximal physical dispersion was obtained through the protocol. As mentioned in Grangeon et al. (2012) both the aggregated and dispersed PSDs are not the same as those obtained by other methods in the literature. Indeed the use of chemical dispersion could have dispersed aggregates much more than the flow shear stress would have

Table 1
Soil characteristics. All contents are in g·kg^{-1}.

Soil	Sampling latitude	Sampling longitude	Clay content (0–2 μm)	Silt content (2–50 μm)	Sand content (50–2000 μm)	Organic carbon content
Molasses	44°11′50″N	06°12′57″E	326	477	197	20
Black marls	44°10′18″N	06°12′56″E	182	566	252	18
Clay soil	44°34′48″N	04°29′44″E	341	413	246	27

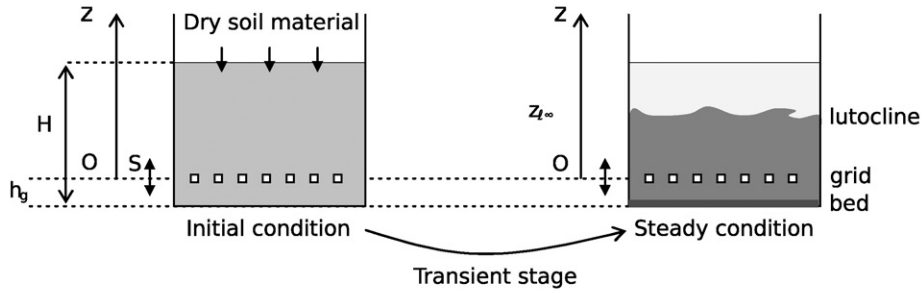

Fig. 1. Grid-stirred experimental setup and procedure. *H*: height of water in the tank, h_g: distance separating the mean grid position from the bottom. *S*: stroke of the oscillations. *O*: origin of the vertical axis (*Z*). $z_{l\infty}$: final lutocline position. Adapted from (Gratiot et al., 2005).

done. An aggregation index *AI* was defined as the relative reduction in volume median particle size between the aggregated and dispersed PSDs (Phillips and Walling, 2005; Grangeon et al., 2014):

$$AI = \frac{d_{50}A - d_{50}D}{d_{50}D} \quad (1)$$

where $d_{50}A$ and $d_{50}D$ are respectively the volume median diameter of the aggregated and the dispersed PSD.

3. Results

3.1. Temporal dynamics of suspended particles

For all the experiments, a bottom deposit and a lutocline appeared immediately after the introduction of the dry material in the tank. As the lutocline acts as a barrier for both turbulence and suspended particles, the relationship between concentration and PSD can be analysed only below the lutocline. The lutocline was affected by waves and plumes and oscillated with an amplitude of roughly 2 cm.

The suspended concentrations at $z = 15$ cm (below the lutocline) remained steady over 40 min for the three materials, except for the clay soil at the highest concentration (Fig. 2a,c,e). This overall stability means that the homogenization within the tank and the adjustment of the suspended concentration to the vertical turbulence profile was rather rapid since the first measurement was done only 1 min after the injection of the amount of soil at the top of the tank.

The suspended concentration below the lutocline increased with the amount of soil introduced (Table 2). Introducing 400 and 1000 g of soil respectively led to SSC close to 1.6 and 5 g L^{-1} for the three soils. However, introducing 2000 g of soil within the tank resulted in concentrations lower than 6.7 g L^{-1} for the clay soil, whilst it rose up to 10 g L^{-1} for the two badland materials.

For all the soils, the lutocline height decreased with the increased amount of introduced material (Table 2). The density gradient through the lutocline becomes stronger which hinders the upward transport of turbulence and particles. The lutocline position also varied depending on the soil type considered. The lutocline height varied from 26 to 19 cm for the two badlands materials, while it did not exceeded 19 cm for the clay soil.

For all materials and concentrations, the median aggregated sizes $d_{50}A$ decreased with time (Fig. 2b,d,f). This decrease was observed during the first ten minutes, the aggregated sizes remaining quasi steady from 10 to 40 min. However this decrease was not similar for all soils and concentrations. The black marl exhibited both the highest size variations with time and the largest differences between the levels of concentrations. For the lower concentration, the $d_{50}A$ decreased from 24 μm to 16 μm between 1 and 40 min (relative variation of −37%) as for the higher concentration it decreased from 16 μm to 13 μm (relative variation of −17%). For the molasses, the relative size variation was higher ranging from −21% to −29%. The smallest size variations with time were observed for the clay soil, with $d_{50}A$ variations during the experiments ranging from −20% to −24%.

3.2. Relationships between particle sizes and concentrations

The first ten minutes were not taken into account in analyzing the size–concentration relationship, because these include multiple interacting processes (such as the settling of the coarsest particles and aggregate breakdown due to the immersion of dry particles). The effect of the concentration was then analyzed during the period from 10 to 40 min, exhibiting little temporal variations. For all the materials, no significant relationship was observed between the 9th decile aggregated size $d_{90}A$ and suspended concentration (Fig. 3a). The size–concentration relationships were significant for the median $d_{50}A$ and first decile $d_{10}A$ aggregated sizes, except for the molasse (Fig. 3b and c). For the clay soil, the $d_{10}A$ and the $d_{50}A$ exhibited respectively a 66% and a 28% decrease as the concentration increased from 2 to 8 g L^{-1}. These decrease were smaller for the two badland materials with values of 16 and 12% respectively. These results suggest that the suspended concentration controls the particle size distribution to some extent, particularly the proportion of the smallest particles, which increases with concentration

Table 2
Summary of the grid stirred experiments principal characteristics.

Experiment label	Soil	Amount of soil introduced in the tank (g)	Time-averaged concentration at $z = 15$ cm (g L^{-1})	Time-averaged aggregated median diameter at $z = 15$ cm (μm)	Lutocline mean position above grid $z_{l\infty}$ (cm)
Marl400	Black marls	400	1.6	18.9	26
Marl1000	Black marls	1000	5.4	18.8	21
Marl2000a	Black marls	2000	10.9	15.2	20
Marl2000b	Black marls	2000	8.5	15.2	20
Molasse400a	Molasses	400	1.6	14.7	26
Molasse400b	Molasses	400	1.6	16.9	25
Molasse1000	Molasses	1000	5.0	15.5	21
Molasse2000a	Molasses	2000	10.5	13.1	19
Molasse2000b	Molasses	2000	9.7	13.2	19
Clay400	Clay soil	400	1.8	63.9	19
Clay1000	Clay soil	1000	5.0	63.8	17
Clay2000	Clay soil	2000	6.7	45.3	15

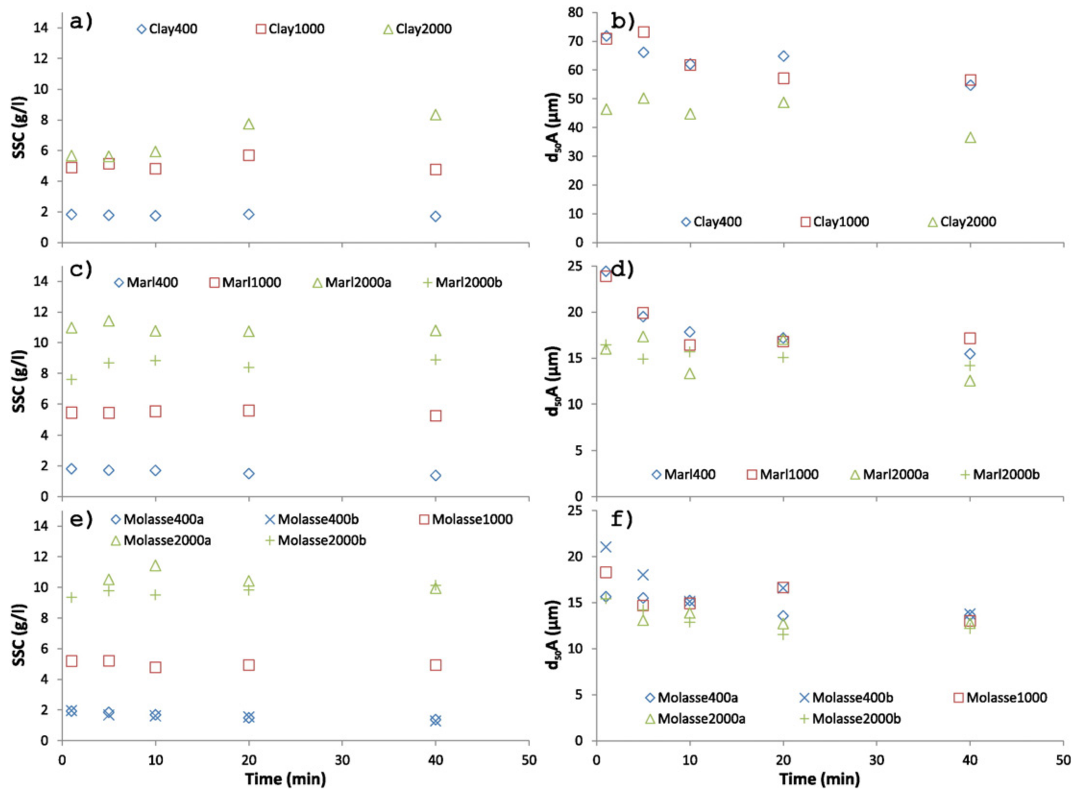

Fig. 2. Time evolution of the suspended concentration (a, c, e) and the median aggregated size (b, d, f). The labels of each time series refer to the characteristics summarized in Table 2.

(Fig. 4). The increase of the proportion of small particles was associated with a decrease of the proportion of the medium particle size classes. Nevertheless, for each soil, the proportion of the largest size class was not affected by concentration as depicted by the nonsignificance of the statistical relationships in Figs. 3a and 4. As previously observed in Fig. 3, these trends were less pronounced for the badland materials than for the clay soil (Fig. 4). It is also worth noting that the limits of the size classes affected by the concentration depend on the considered soil.

4. Discussion

4.1. Mechanisms responsible for the size–concentration relationships

As shown in Table 2, the height of the lutocline decreased as the amount of dry material introduced in the grid tank increased. This was due to the turbulence damping that occurred at a lower elevation for a more concentrated suspension (Michallet and Mory, 2004). Given that the absolute depth of sampling remained unchanged (15 cm) for all the experiments, the relative distance below the lutocline ranged from 4–5 cm for the two badlands materials to almost 0 for the clay soil at the highest concentration. Thus we first analysed if the variations of the lutocline position with concentration could be responsible for the size–concentration relationships.

The effect of the lutocline on the suspended material is illustrated in Fig. 5, which shows aggregated particle size distributions for each soil and two contrasted experiments in terms of suspended concentrations. The particle size distributions measured at $t = 40$ min are shown for two depths, one below the lutocline ($z = 15$ cm), and one above the lutocline for the largest concentration ($z = 20$ cm or $z = 25$ cm). The samples collected at 20 or 25 cm were systematically reduced in large particles in comparison with those collected at 15 cm. The complete or quasi-complete disappearance of the largest size class (larger than 100 µm for the two badland materials and larger than 200 µm for the clay soil) indicates that the stratification effects within the tank strongly affect the largest particles. The PSD differences were more pronounced for the experiments performed at high concentrations (2000 g of material introduced), showing that the lutocline acts as a strong barrier for the heaviest particles. For the experiments at low concentration, both measurement depths remained below or close to the lutocline and a weak stratification was observed. Lower turbulent activity at $z = 20$ cm led to a slight reduction in particle sizes compared to that measured at $z = 15$ cm. Focusing on the samples collected at $z = 15$ cm, the size–concentration relationship was limited to small and medium size classes. As shown in Fig. 4, the largest particle size class (i.e. >63 µm particles for the two badland materials and >250 µm for the clay soil) did not exhibit any significant correlation with the concentration ($R^2 < 0.05$). This further indicates that the largest size class was equally present in all the samples collected at $z = 15$ cm regardless of the concentration. Consequently, the size–concentration relationship observed at $z = 15$ cm for the other classes cannot be attributed to stratification effects, as these would have also affected the largest particles. The variations in proportion of the medium and small size classes observed in Fig. 4 were therefore interpreted as a direct effect of the suspended concentration on the size of the particles.

Fig. 6a emphasizes that all suspended sediment samples were aggregated with aggregation index values ranging from $AI = 0.3$ in average for the two badland materials to $AI = 0.85$ for the clay soil. An example of aggregate breakdown during sonication within the laser sizer is presented in Fig. 6b for the clay soil. The disaggregation dynamics is presented for the samples collected at 15 cm for the lower (Clay400) and higher (Clay2000) concentrations. After 10 min of sonication and high stirring, both samples exhibited similar particle size distributions, with all the particles larger than 100 µm being disaggregated. This confirms that the primary particles forming the suspended aggregates did not vary from one experiment to another, i.e. from one concentration to another. The same behaviour during sonication was observed for the marl and molasse materials (not shown). Nevertheless the low aggregation index (from 0.2 to 0.4) of those materials led to smaller variations in particle sizes.

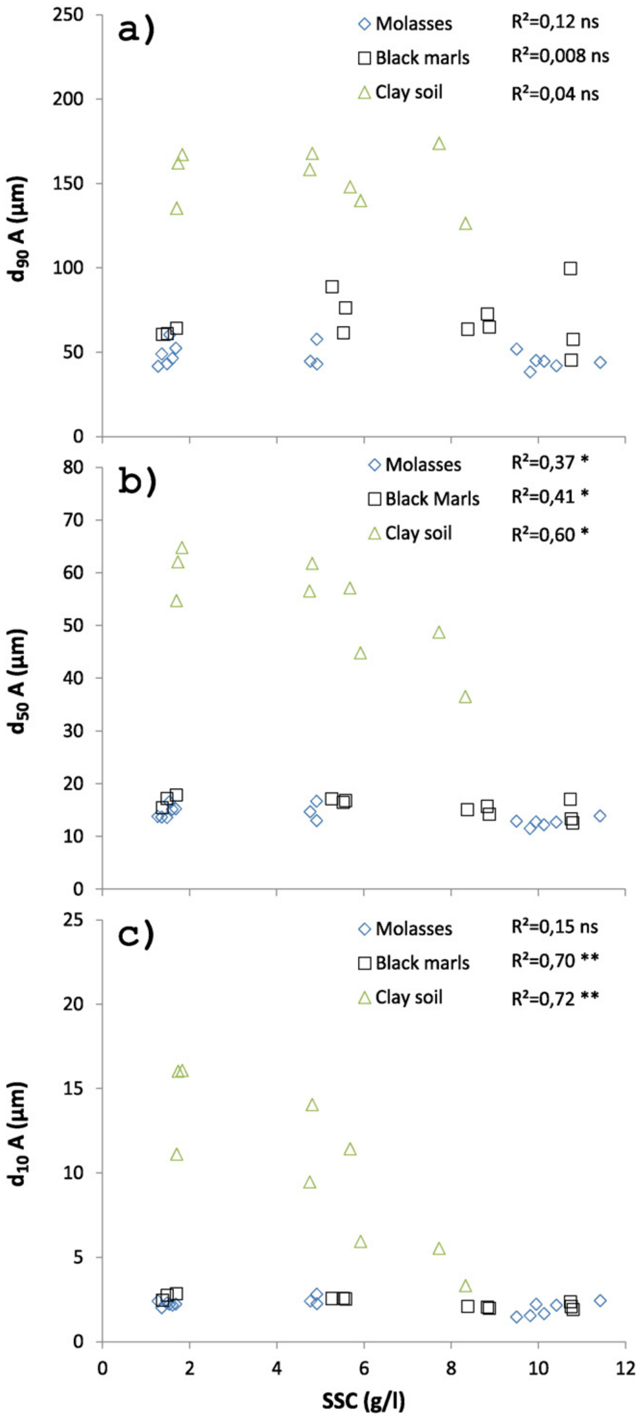

Fig. 3. Scatter plot of suspended concentration and $d_{90}A$ (a), $d_{50}A$ (b) $d_{10}A$ (c). For each dataset, the coefficient of determination (R^2) of a linear regression and its level of significance (p-value) is presented in the legend (ns: non significant; *: $p < 0.05$; **: $p < 0.01$).

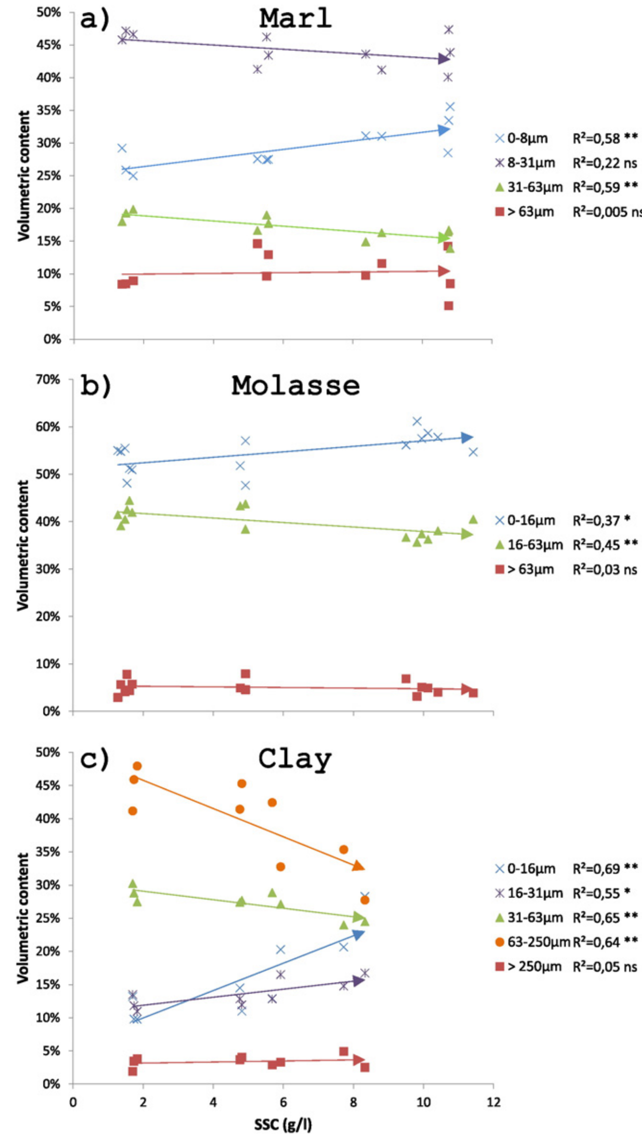

Fig. 4. Scatter plot of the suspended concentration and the volumetric amount of particles for various size classes of the aggregated size distribution for the a) black marls, b) molasses and c) clay soil. The lines correspond to linear regressions. The coefficient of determination of each regression (R^2) and its level of significance (p-value) are presented in the legend (ns: non significant; *: $p < 0.05$; **: $p < 0.01$).

The concentration was mainly found to increase the smallest size proportion whilst most of the large aggregates remained intact. This dynamics could be interpreted as the signature of abrasion, generating small particles from the periphery of medium-size aggregates (Legout et al., 2005). Abrasion is a cumulative process, fine fragments quantity being proportional to the cumulative mechanical energy applied to the sample (Le Bissonnais, 1988). The experiments conducted by Larionov et al. (2007) and Wang et al. (2012, 2013, 2014) aiming at exploring the evolution of aggregate properties within runoff through flume experiments already mentioned that surface aggregate abrasion exerts a main control on the particle size during their transport. Those studies show that abrasion of soil aggregates differs from mineral particle abrasion and depends on the strength of the aggregates. As the sampling location at $z = 15$ cm was never above the lutocline, the turbulence at this elevation could be considered identical for all experiments (Gratiot et al., 2005). Increasing the suspended concentration led to more frequent collisions between particles (Abrahamson, 1975). If the probability of breakdown or abrasion during a collision is higher than the probability of cohesion, the statistical effect of an increasing collision number is a decreased mean particle size (Winterwerp, 1999). Our results suggest that in case of soil aggregates, collision were mainly destructive and led to particle surface abrasion.

4.2. Respective effects of soil type, temporal dynamics and concentration on particle sizes

In the present study, the soil type was the dominant factor controlling particle size. The suspended concentration and the temporal dynamics within the flow were of second order. Indeed the two

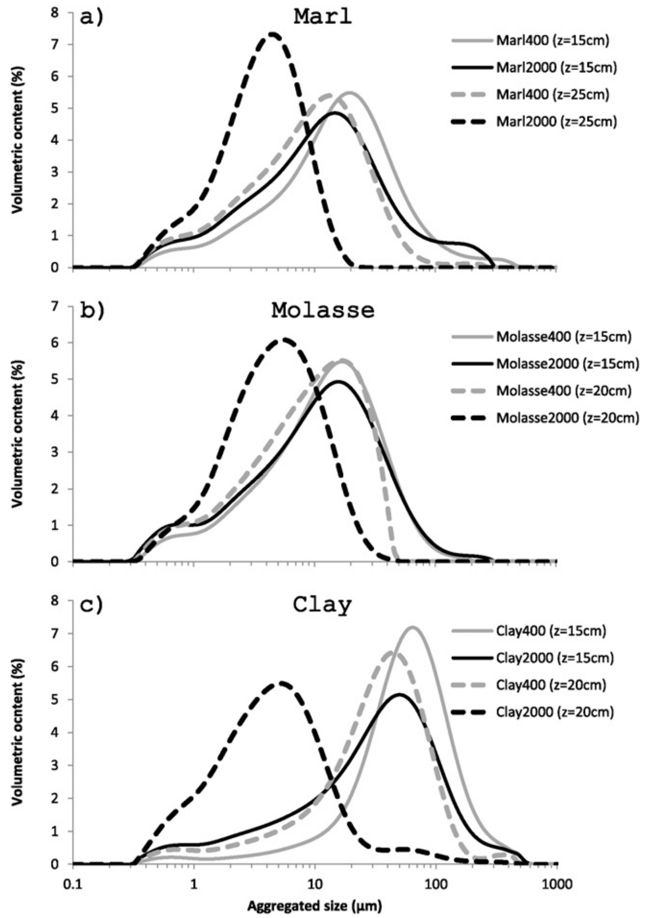

Fig. 5. Aggregated particle size distributions for a) black marls, b) molasses and c) clay soil. For each soil, two levels of concentrations are presented at two sampling distances above the grid.

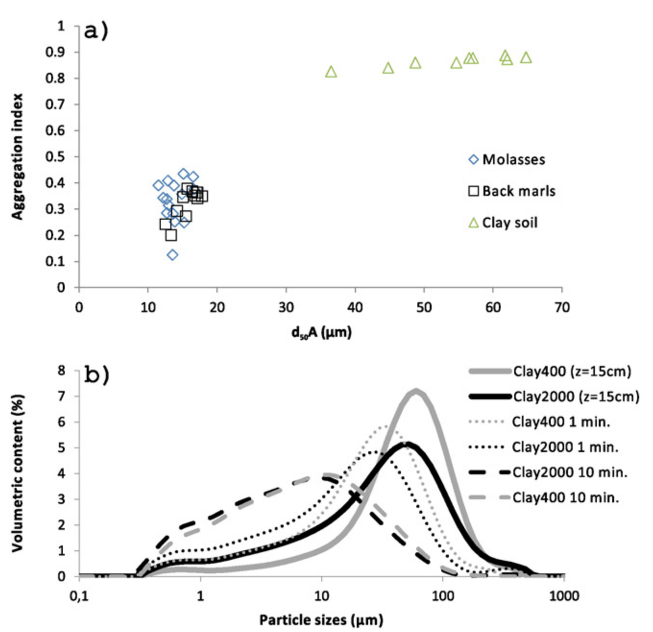

Fig. 6. a) Scattering of the aggregation indexes measured on samples collected in the grid tank after 10, 20 and 40 min for the whole set of experiments. b) Dynamics of aggregate breakdown within the laser sizer for the clay soil. The initial particle size distribution and the ones after 1 and 10 min of strong sonication and stirring are shown for Clay400 and Clay2000.

badlands materials exhibited similar trends with aggregated d_{50} between 10 and 20 μm whereas the clay soil had aggregated d_{50} between 35 and 70 μm (Fig. 6). The clay soil results from a longer pedogenesis process than the badland materials. Its high aggregated d_{50} was also associated with high aggregation indexes and to slightly higher organic matter content. While it was not possible in this study to precisely identify the properties that were responsible for the higher particle strengths of the clay soil, organic matter is recognized to glue small particles within aggregates, thus increasing their stability (Chenu et al., 2000; Cosentino et al., 2006; Leppard and Droppo, 2005). Transmission electronic microscopy observations done by Grangeon et al. (2014) confirmed that the black marls and the molasses showed very little microbial or organic material within the matrix of the particles. This would also be consistent with the higher resistance of the clay soil aggregates to the slaking mechanism due to air entrapment during the early times of the experiment when dry aggregates were suddenly immersed in the water.

In experiments conducted in an annular flume with the same materials, (Grangeon et al. (2014) also observed that the soil type was the first controlling parameter during the first stages of their experiments, when the shear stress was increasing to simulate the rising limb of an hydrograph. Particularly they showed that an increase in the shearing level enhances disaggregation. The present study shows that an increase of suspended concentration also enhances disaggregation through particle surface abrasion, leading to an increased proportion of small particles. Grangeon et al. (2014) also noticed that the small particles generated by disaggregation during the rising limb of the hydrograph were subjected to flocculation during the falling limb. This suggests that the higher amounts of small particles in the suspension generated by abrasion at high concentration could be reduced later if the hydrodynamic conditions change (i.e. become less turbulent) due to flocculation of the small particles. By reducing the size of the aggregates, the process of abrasion promotes their distance of transport downstream and thus potentially modifies the areas of deposition. This process may also have implications on the nutrient or contaminant fluxes as adsorption is known to occur mainly on fine particles. Together with the results of Grangeon et al. (2014), the results of this study highlight the potential issues of using conservative particle sizes to model the erosion-transport of sediments in upland environments. In lowlands and estuarine environments, additional factors such as microbial activity (Leppard and Droppo, 2005) and ionic strength (Migniot, 1968; Thill et al., 2001) are likely of uppermost importance.

5. Conclusions

Three soil materials were introduced in a grid stirred tank in order to analyse the respective role of the soil type and the suspended concentration on the size of particles. A steady suspended concentration was reached less than one minute after the introduction of the dry material within the turbulent flow. The particle sizes decreased during the first 10 min of shearing, and remained approximately constant for the rest of the experiments. The particle size distributions between 10 and 40 min for the different soils and concentrations were compared. Increasing the suspended concentrations led to a decrease of the proportion of the medium size particles and to an associated increase of the proportion of the smallest particles. The proportion of large aggregates exhibited no correlation with concentration. This indicates that size variations due to the difference of suspended concentration was mainly due to an enhanced abrasion of aggregate surfaces. Similar trends were observed with increasing the shearing levels by Grangeon et al. (2014).

Even though a dependence of the particle sizes to the suspended concentration and shearing level was observed, the initial soil characteristics remained the main controlling parameter of the particle size after 40 min within the turbulent environment.

Acknowledgments

This work has been funded by the French Agence Nationale de la Recherche (ANR-12-JS06-0006) and Institut National des Sciences de l'Univers (EC2CO BIOHEFECT). We are also grateful to Andrew Manning, Magalie Jodeau, Germain Antoine and Jean-Marc Barnoud for their participation to the laboratory experiments. LTHE is part of Labex OSUG@2020 (ANR10 LABX56).

References

Abrahamson, J., 1975. Collision rates of small particles in a vigorously turbulent fluid. Chem. Eng. Sci. 30, 1371–1379. http://dx.doi.org/10.1016/0009-2509(75)85067-6.

Andrews, S., Nover, D., Schladow, S.G., 2010. Using laser diffraction data to obtain accurate particle size distributions: the role of particle composition. Limnol. Oceanogr. Methods 8, 507–526. http://dx.doi.org/10.4319/lom.2010.8.507.

Boardman, J., 2006. Soil erosion science: reflections on the limitations of current approaches. Catena 68, 73–86. http://dx.doi.org/10.1016/j.catena.2006.03.007.

Boudevillain, B., Delrieu, G., Galabertier, B., Bonnifait, L., Bouilloud, L., Kirstetter, P.E., Mosini, M.L., 2011. The Cévennes-Vivarais Mediterranean Hydrometeorological Observatory database. Water Resour. Res. 47, W07701. http://dx.doi.org/10.1029/2010WR010353.

Chenu, C., Le Bissonnais, Y., Arrouays, D., 2000. Organic matter influence on clay wettability and soil aggregate stability. Soil Sci. Soc. Am. J. 64, 1479–1486.

Collins, A.L., Walling, D.E., Leeksz, G.J.L., 2005. Storage of fine-grained sediment and associated contaminants within the channels of lowland permeable catchments in the UK. In: Walling, D.E., Horowitz, A.J. (Eds.), Sediment Budgets 1 vol. 291. Int Assoc Hydrological Sciences, Wallingford, pp. 259–268.

Cosentino, D., Chenu, C., Le Bissonnais, Y., 2006. Aggregate stability and microbial community dynamics under drying–wetting cycles in a silt loam soil. Soil Biol. Biochem. 38, 2053–2062. http://dx.doi.org/10.1016/j.soilbio.2005.12.022.

De Vente, J., Poesen, J., Verstraeten, G., Govers, G., Vanmaercke, M., Van Rompaey, A., Arabkhedri, M., Boix-Fayos, C., 2013. Predicting soil erosion and sediment yield at regional scales: where do we stand? Earth Sci. Rev. 127, 16–29. http://dx.doi.org/10.1016/j.earscirev.2013.08.014.

Droppo, I.G., 2004. Structural controls on floc strength and transport. Can. J. Civ. Eng. 31, 569–578. http://dx.doi.org/10.1139/l04-015.

Droppo, I., Nackaerts, K., Walling, D., Williams, N., 2005. Can flocs and water stable soil aggregates be differentiated within fluvial systems? Catena 60, 1–18. http://dx.doi.org/10.1016/j.catena.2004.11.002.

Dyer, K.R., 1989. Sediment processes in estuaries: future research requirements. J. Geophys. Res. Oceans 94, 14327–14339.

Graham, G.W., Davies, E.J., Nimmo-Smith, W.A.M., Bowers, D.G., Braithwaite, K.M., 2012. Interpreting LISST-100X measurements of particles with complex shape using digital in-line holography. J. Geophys. Res. Oceans 117, C05034. http://dx.doi.org/10.1029/2011JC007613.

Grangeon, T., Droppo, I.G., Legout, C., Esteves, M., 2014. From soil aggregates to riverine flocs: a laboratory experiment assessing the respective effects of soil type and flow shear stress on particles characteristics. Hydrol. Process. 28, 4141–4155. http://dx.doi.org/10.1002/hyp.9929.

Grangeon, T., Legout, C., Esteves, M., Gratiot, N., Navratil, O., 2012. Variability of the particle size of suspended sediment during highly concentrated flood events in a small mountainous catchment. J. Soils Sediments 12, 1549–1558. http://dx.doi.org/10.1007/s11368-012-0562-5.

Gratiot, N., Manning, A.J., 2004. An experimental investigation of floc characteristics in a diffusive turbulent flow. J. Coast. Res. 105–113.

Gratiot, N., Michallet, H., Mory, M., 2005. On the determination of the settling flux of cohesive sediments in a turbulent fluid. J. Geophys. Res. 110. http://dx.doi.org/10.1029/2004JC002732.

Hopfinger, E.J., Toly, J.A., 1976. Spatially decaying turbulence and its relation to mixing across density interfaces. J. Fluid Mech. 78, 155–175. http://dx.doi.org/10.1017/S0022112076002371.

Jarvis, P., Jefferson, B., Gregory, J., Parsons, S., 2005. A review of floc strength and breakage. Water Res. 39, 3121–3137. http://dx.doi.org/10.1016/j.watres.2005.05.022.

Jetten, V., de Roo, A., Favis-Mortlock, D., 1999. Evaluation of field-scale and catchment-scale soil erosion models. Catena 37, 521–541. http://dx.doi.org/10.1016/S0341-8162(99)00037-5.

Jetten, V., Govers, G., Hessel, R., 2003. Erosion models: quality of spatial predictions. Hydrol. Process. 17, 887–900. http://dx.doi.org/10.1002/hyp.1168.

Jones, A., Panagos, P., Barcelo, S., Bouraoui, F., Bosco, C., Dewitte, O., Gardi, C., Hervás, J., Hiederer, R., Jeffery, S., Montanarella, L., Penizek, V., Tóth, G., Van Den Eeckhaut, M., Van Liedekerke, M., Verheijen, F., Yigini, Y., 2012. The State of Soil in Europe — A Contribution of the JRC to the European Environment Agency's Environment State and Outlook Report — SOER 2010. Publications Office of the European Union.

Larionov, G.A., Bushueva, O.G., Dobrovol'skaya, N.G., Kiryukhina, Z.P., Litvin, L.F., Maksimova, I.A., 2007. Destruction of soil aggregates in slope flows. Eurasian Soil Sci. 40, 1128–1134. http://dx.doi.org/10.1134/S1064229307100110.

Le Bissonnais, Y., 1988. Comportement d'agrégats terreux soumis à l'action de l'eau: analyse des mécanismes de désagrégation. Agronomie 8, 915–924.

Le Bissonnais, Y., Blavet, D., De Noni, G., Laurent, J.Y., Asseline, J., Chenu, C., 2007. Erodibility of Mediterranean vineyard soils: relevant aggregate stability methods and significant soil variables. Eur. J. Soil Sci. 58, 188–195. http://dx.doi.org/10.1111/j.1365-2389.2006.00823.x.

Legout, C., Leguedois, S., Le Bissonnais, Y., 2005. Aggregate breakdown dynamics under rainfall compared with aggregate stability measurements. Eur. J. Soil Sci. 56, 225–238. http://dx.doi.org/10.1111/j.1365-2389.2004.00663.x.

Legout, C., Poulenard, J., Nemery, J., Navratil, O., Grangeon, T., Evrard, O., Esteves, M., 2013. Quantifying suspended sediment sources during runoff events in headwater catchments using spectrocolorimetry. J. Soils Sediments 13, 1478–1492. http://dx.doi.org/10.1007/s11368-013-0728-9.

Leppard, G.G., Droppo, I.G., 2005. Overview of flocculation processes in freshwater ecosystems. In: Droppo, I.G., Leppard, G.G., Liss, S.N., Milligan, T.G. (Eds.), Flocculation in Natural and Engineered Environmental Systems. Crc Press-Taylor & Francis Group, Boca Raton, pp. 25–46.

Matsunaga, N., Sugihara, Y., Komatsu, T., Masuda, A., 1999. Quantitative properties of oscillating-grid turbulence in a homogeneous fluid. Fluid Dyn. Res. 25, 147. http://dx.doi.org/10.1016/S0169-5983(98)00034-3.

Michallet, H., Mory, M., 2004. Modelling of sediment suspensions in oscillating grid turbulence. Fluid Dyn. Res. 35, 87–106. http://dx.doi.org/10.1016/j.fluiddyn.2004.04.004.

Migniot, C., 1968. Etude des propriétés physiques de différents sédiments très fins et de leur comportement sous des actions hydrodynamiques. La Houille Blanche 7, 591–620. http://dx.doi.org/10.1051/lhb/1968041.

Navratil, O., Esteves, M., Legout, C., Gratiot, N., Nemery, J., Willmore, S., Grangeon, T., 2011. Global uncertainty analysis of suspended sediment monitoring using turbidimeter in a small mountainous river catchment. J. Hydrol. 398, 246–259. http://dx.doi.org/10.1016/j.jhydrol.2010.12.025.

Navratil, O., Evrard, O., Esteves, M., Legout, C., Ayrault, S., Némery, J., Mate-Marin, A., Ahmadi, M., Lefèvre, I., Poirel, A., Bonté, P., 2012. Temporal variability of suspended sediment sources in an alpine catchment combining river/rainfall monitoring and sediment fingerprinting. Earth Surf. Process. Landf. 37, 828–846. http://dx.doi.org/10.1002/esp.3201.

Owens, P.N., Batalla, R.J., Collins, A.J., Gomez, B., Hicks, D.M., Horowitz, A.J., Kondolf, G.M., Marden, M., Page, M.J., Peacock, D.H., Petticrew, E.L., Salomons, W., Trustrum, N.A., 2005. Fine-grained sediment in river systems: environmental significance and management issues. River Res. Appl. 21, 693–717. http://dx.doi.org/10.1002/rra.878.

Phillips, J.M., Walling, D.E., 2005. Intra-storm and seasonal variations in the effective particle size characteristics and effective particle density of fluvial suspended sediment in the Exe Basin, Devon, United Kingdom. In: Droppo, I.G., Leppard, G.G., Liss, S.N., Milligan, T.G. (Eds.), Intra-storm and Seasonal Variations in the Effective Particle Size Characteristics and Effective Particle Density of Fluvial Suspended Sediment in the Exe Basin, Devon, United Kingdom. Crc Press-Taylor & Francis Group, Boca Raton, pp. 47–70.

Thill, A., Moustier, S., Garnier, J.M., Estournel, C., Naudin, J.J., Bottero, J.Y., 2001. Evolution of particle size and concentration in the Rhône river mixing zone: influence of salt flocculation. Cont. Shelf Res. 21, 2127–2140. http://dx.doi.org/10.1016/S0278-4343(01)00047-4.

Wainwright, J., Parsons, A.J., Müller, E.N., Brazier, R.E., Powell, D.M., Fenti, B., 2008. A transport-distance approach to scaling erosion rates: 1. Background and model development. Earth Surf. Process. Landf. 33, 813–826. http://dx.doi.org/10.1002/esp.1624.

Wang, J.G., Li, Z.X., Cai, C.F., Ma, R.M., 2014. Particle size and shape variation of Ultisol aggregates affected by abrasion under different transport distances in overland flow. Catena 123, 153–162. http://dx.doi.org/10.1016/j.catena.2014.07.020.

Wang, J.G., Li, Z.X., Cai, C.F., Yang, W., 2012. Effects of transport distance and flow discharge of overland flow on destruction of Ultisol aggregates. Particuology 10, 607–613. http://dx.doi.org/10.1016/j.partic.2011.06.013.

Wang, J.G., Li, Z.X., Cai, C.F., Yang, W., Ma, R.M., Zhang, G.B., 2013. Effects of stability, transport distance and two hydraulic parameters on aggregate abrasion of Ultisols in overland flow. Soil Tillage Res. 126, 134–142. http://dx.doi.org/10.1016/j.still.2012.09.005.

Williams, N.D., Walling, D.E., Leeks, G.J.L., 2008. An analysis of the factors contributing to the settling potential of fine fluvial sediment. Hydrol. Process. 22, 4153–4162. http://dx.doi.org/10.1002/hyp.7015.

Winterwerp, J.C., 1999. On the Dynamics of High-concentrated Mud Suspensions. Delft University of Technology, Faculty of Civil Engineering and Geosciences.

Winterwerp, J.C., 2001. Stratification effects by cohesive and noncohesive sediment. J. Geophys. Res. Oceans 106, 22559–22574. http://dx.doi.org/10.1029/2000JC000435.